Inorganic Chemistry

Article

pubs.acs.org/IC

Molecular and Electronic Structures of Mononuclear and Dinuclear Titanium Complexes Containing π-Radical Anions of 2,2′-Bipyridine and 1,10-Phenanthroline: An Experimental and DFT Computational Study

Carina Wolff,[†] Andreas Gottschlich,[†] Jason England,[‡,§] Karl Wieghardt,*[,‡] Wolfgang Saak,[†] Detlev Haase,[†] and Rüdiger Beckhaus*[,†]

[†]Institute of Chemistry, Carl von Ossietzky University of Oldenburg, D-26111 Oldenburg, Germany

[‡]Max Planck Institute for Chemical Energy Conversion, Stiftstrasse 34−36, D-45470 Mülheim an der Ruhr, Germany

Supporting Information

ABSTRACT: Whereas reaction of $[(\eta^5\text{-Cp}^*)\text{Ti}^{IV}\text{Cl}_3]^0$ (**1**) with 2 equiv of neutral 2,2′-bipyridine (bpy) and 1.5 equiv of magnesium in tetrahydrofuran affords the mononuclear complex $[(\eta^5\text{-Cp}^*)\text{Ti}^{III}(\text{bpy}^\bullet)_2]^0$ (**2**), performing the same reaction with only 1 equiv each of magnesium and bpy provides the dinuclear complex $[\{(\eta^5\text{-Cp}^*)\text{Ti}(\mu\text{-Cl})(\text{bpy}^\bullet)\}_2]^0$ (**3**). Conducting the latter reaction using 1,10-phenanthroline (phen) in place of bpy resulted in formation of dinuclear $[\{(\eta^5\text{-Cp}^*)\text{Ti}(\mu\text{-Cl})(\text{phen}^\bullet)\}_2]^0$ (**4**). The structures of **2**, **3**, and **4** have all been determined by high-resolution X-ray crystallography at 153 K; the $C_{py}-C_{py}$ distances of 1.420(3) and 1.431(4) Å in the *N*,*N*′-coordinated bpy ligands of **2** and **3**, respectively, are indicative of the presence of $(\text{bpy}^\bullet)^{1-}$ ligands, rather than neutral (bpy^0). The electronic spectra (300−1600 nm) of these two complexes are similar in form, and contain intense $\pi \rightarrow \pi^*$ transitions associated with the $(\text{bpy}^\bullet)^{1-}$ radical anion. Temperature dependent magnetic susceptibility measurements (4−300 K) show that mononuclear **2** possesses a temperature independent magnetic moment of 1.73 μ_B, which is indicative of an $S = {}^1/_2$ ground state. Broken symmetry density functional theory (BS-DFT) calculations yield a picture consistent with the experimental findings, in which the central Ti atom possesses a +3 oxidation state and is coordinated by a η^5-Cp* ligand and two $(\text{bpy}^\bullet)^{1-}$. Strong intramolecular *antiferromagnetic* coupling of these three unpaired spins, one each on the Ti^{III} center and on the two $(\text{bpy}^\bullet)^{1-}$ ligands, affords the experimentally observed doublet ground state. The magnetic susceptibility measurements for dinuclear **3** and **4** display weak but significant *ferromagnetic* coupling, and indicate that these complexes possess $S = 1$ ground states. The mechanism of the spin coupling phenomenon that yields the observed behavior was analyzed using BS-DFT calculations, and it was discovered that the tight π-stacking of the *N*,*N*′-coordinated $(\text{bpy}^\bullet)^{1-}/(\text{phen}^\bullet)^{1-}$ ligands in these two complexes results from direct overlap of their SOMOs and formation of a two-electron multicentered bond. This yields a diamagnetic $\{(\text{bpy})_2\}^{2-}/\{(\text{phen})_2\}^{2-}$ bridging unit whose doubly occupied HOMO is spread equally over both ligands. The two remaining unpaired electrons, one at each Ti^{III} center, couple weakly in a ferromagnetic fashion to yield the experimentally observed $S = 1$ ground states.

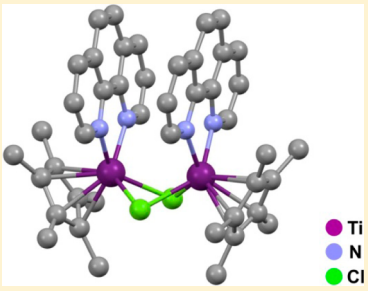

INTRODUCTION

The redox active nature of 2,2′-bipyridine (bpy) has long been recognized. However, it is only relatively recently, upon the publication of high-resolution X-ray crystal structures of alkali metal salts of the π-radical $(\text{bpy}^\bullet)^{1-}$ monoanion and diamagnetic $(\text{bpy}^{2-})^{2-}$ dianion (Chart 1),[1,2] and studies containing extensive DFT calculations for series of transition metal complexes,[3,4] that it has been shown that the bpy ligand structural parameters can be used to discern its *discrete* redox state in any given compound. This has allowed definitive assignment of electronic structure in a wide array of transition metal complexes, where it was often previously unknown, implied, or incorrectly assigned.

For instance, the molecular and electronic structures of the four members of the electron transfer series of the mononuclear *bent*-titanocene complexes $[(\eta^5\text{-Cp})_2\text{Ti}(\text{bpy})]^{1-,0,1+,2+}$ (Cp^- represents the cyclopentadienyl anion, Chart 1) have been experimentally investigated using a combination of X-ray crystallography, UV−vis and EPR spectroscopies, and magnetochemistry.[5−7] These studies suggested that the bpy ligand is redox active, but it is only with recent augmentation of these studies via calculations performed using density functional theory (DFT)[4a] and ab initio methods[8] that unequivocal assignment of their electronic structures has proven possible. It was concluded that the $S = {}^1/_2$ monoanion $[(\eta^3\text{-Cp})(\eta^5\text{-Cp})\text{Ti}^{III}(\text{bpy}^{2-})]^{1-}$ possesses a metal-centered unpaired spin; the neutral species $[(\eta^5\text{-Cp})_2\text{Ti}^{III}(\text{bpy}^\bullet)]^0$ has an open-shell singlet diradical ground state attained via antiferromagnetic coupling ($J_{exp} = -300\ \text{cm}^{-1}$) of the metal-centered unpaired spin with that of the $(\text{bpy}^\bullet)^{1-}$ π-radical ($\hat{H} = -2JS_{Ti}\cdot S_L$; $S_{Ti} = S_L = {}^1/_2$); $[(\eta^5\text{-Cp})_2\text{Ti}^{III}(\text{bpy}^0)]^{1+}$

Received: February 5, 2015
Published: April 30, 2015

DOI: 10.1021/acs.inorgchem.5b00285
Inorg. Chem. 2015, 54, 4811−4820

Chart 1. Complexes, Spin States, and Ligands Featured in This Work

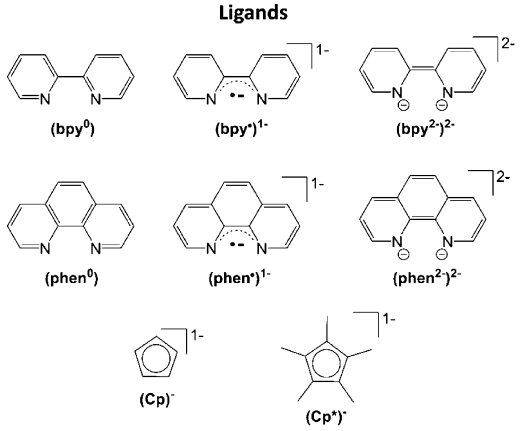

Complexes

$[(\eta^5\text{-Cp*})Ti^{IV}Cl_3]^0$	(S = 0)	**(1)**
$[(\eta^5\text{-Cp*})Ti^{III}(bpy^{\bullet})_2]^0$	(S = 1/2)	**(2)**
$[\{(\eta^5\text{-Cp*})Ti^{III}(\mu\text{-Cl})(bpy^{\bullet})\}_2]^0$	(S = 1)	**(3)**
$[\{(\eta^5\text{-Cp*})Ti^{III}(\mu\text{-Cl})(phen^{\bullet})\}_2]^0$	(S = 1)	**(4)**
$[\{(\eta^5\text{-Cp})_2Ti^{III}(\mu\text{-F})\}_2]^0$	(S = 0)	**(5)**
$[\{(\eta^5\text{-Cp})_2Ti^{III}(\mu\text{-Cl})\}_2]^0$	(S = 0)	**(6)**
$[\{(\eta^5\text{-Cp*})Sc^{III}(\mu\text{-Cl})(bpy^{\bullet})\}_2]^0$	(S = 0)	**(7)**

has a metal-centered doublet ($S = {}^1/_2$) ground state; and oxidation of the monocation to the corresponding dication is metal-centered and yields diamagnetic $[(\eta^5\text{-Cp})_2Ti^{IV}(bpy^0)]^{2+}$.

Extension of such studies to dinuclear complexes, particularly elucidation of the impact of ligand-centered unpaired spin upon magnetic interactions between the two metal centers, represents an intriguing proposition. To this end, we have synthesized mononuclear $[(\eta^5\text{-Cp*})Ti(bpy)_2]^0$ (**2**), and the closely related dinuclear $[\{(\eta^5\text{-Cp*})Ti(\mu\text{-Cl})(bpy)\}_2]^0$ (**3**) and $[\{(\eta^5\text{-Cp*})Ti(\mu\text{-Cl})(phen)\}_2]^0$ (**4**; phen = 1,10-phenanthroline), all from the monocyclopentadienyl derivative $[(\eta^5\text{-Cp*})TiCl_3]^0$ (**1**)[9] (Chart 1). The electronic structures of these three complexes were investigated and definitively assigned using a combination of high-resolution X-ray crystallography, UV−vis spectroscopy, magnetic susceptibility measurements, and density functional theory (DFT) calculations. Interpretation of these results within a context provided by the *N*-heterocycle free dinuclear diamagnetic complexes $[\{(\eta^5\text{-Cp})_2Ti^{III}(\mu\text{-F})\}_2]^0$ (**5**) and $[\{(\eta^5\text{-Cp})_2Ti^{III}(\mu\text{-Cl})\}_2]^0$ (**6**),[10,11] and Tilley's scandium complex $[\{(\eta^5\text{-Cp*})Sc(\mu\text{-Cl})(bpy)\}_2]^0$ (**7**, S = 0),[12] which is structurally similar to **3** and **4**, allowed for rationalization of their magnetic properties and highlights the pivotal importance of strong bpy/phen $\pi-\pi$ stacking interactions in these systems.

EXPERIMENTAL SECTION

General Information. All operations were performed in a nitrogen atmosphere with rigorous exclusion of oxygen and moisture using standard Schlenk techniques and an inert atmosphere glovebox. $[(\eta^5\text{-Cp*})TiCl_3]^0$ (**1**) was prepared according to a literature procedure;[9] the ligands bpy (2,2′-bipyridine) and phen (1,10-phenanthroline) were purchased from Sigma-Aldrich and used as received. Solvents were distilled under a nitrogen atmosphere, over Na/K alloy and benzophenone. Electron impact (EI) mass spectra were taken on a Finnigan-MAT 95 spectrometer. IR spectra were recorded on a Bruker Vektor 22 spectrometer using KBr pellets. Melting points were determined using a MEL-Temp by Laboratory Devices (Cambridge, U.K.), and elemental analyses were carried out by using an EA Euro 3000 from EuroVector (Milan, Italy). Single crystal X-ray diffraction experiments were performed using a STOE IPDS and a Bruker AXS X8 Apex II diffractometer with graphite-monochromated Mo Kα radiation (λ = 0.710 73 Å). The structures were solved by direct phase determination and refined by full-matrix least-squares techniques against F^2 with the SHELXL-97 program system.[13] Electronic spectra were recorded with a PerkinElmer Lambda 19 double-beam spectrophotometer (200−2100 nm). Variable temperature (4−300 K) magnetization data were recorded in a 1 T magnetic field using a SQUID magnetometer (MPMS quantum design).

Synthesis of $[(\eta^5\text{-Cp*})Ti(bpy)_2]^0$ (2). Complex **1** (100 mg, 0.34 mmol), magnesium metal (12.8 mg, 0.51 mmol), and bpy (107.8 mg, 0.69 mmol) were stirred together in 40 mL of THF at room temperature for 64 h, during which time the color of the solution turned from orange to deep brown. Subsequently, the solvent was removed under vacuum and the resulting residue extracted by stirring in 40 mL of toluene at room temperature for 2 h. Filtration, followed by removal of all volatiles from the filtrate, yielded the product as a black solid in 51% yield (87.5 mg, 0.18 mmol). Single crystals of **2** suitable for X-ray diffraction were obtained from a saturated THF solution of complex after storage for several days at −15 °C. Mp: 200 °C (dec). IR (KBr; cm^{-1}): $\tilde{\nu}$ 2965 (m), 2897 (m), 2866 (m), 1544 (s), 1500 (s), 1460 (m), 1445 (s), 1366 (m), 1321 (m), 1285 (s), 1256 (m), 1215 (m), 1145 (m), 1086 (m), 1017 (w), 957 (s), 849 (s), 754 (m), 723 (m), 651 (w). MS (EI, 70 eV) m/z (%): 156 (100) $[bpy]^+$, 135 (30) $[Cp^*]^+$. Anal. Calcd for $C_{30}H_{31}N_4Ti$: C, 72.72; H, 6.31; N, 11.31. Found: C, 72.58; H, 6.19; N, 11.08.

Synthesis of $[\{Cp^*Ti(\mu\text{-Cl})(bpy)\}_2]^0$ (3). Equimolar quantities of **1** (100 mg, 0.34 mmol), magnesium metal (8.4 mg, 0.34 mmol), and bpy (53.9 mg, 0.34 mmol) were stirred together in 20 mL of THF at room temperature for 40 h. During this time the color of the solution turned from orange to deep blue. Subsequent workup was performed in a fashion analogous to that of complex **2** and yielded **3** as a black solid in 93% yield (120 mg, 0.16 mmol). Single crystals of **3** suitable for X-ray diffraction were grown from a saturated *n*-hexane solution of complex after several days at 4 °C. Mp: 150 °C (dec). IR (KBr; cm^{-1}): $\tilde{\nu}$ 2962 (m), 2904 (m), 1572 (m), 1521 (m), 1449 (m), 1413 (s), 1374 (m), 1334 (m), 1260 (m), 1235 (m), 1150 (m), 1090 (m), 1022 (m), 962 (s), 795 (w), 755 (w), 730 (w), 693 (m), 647 (w), 615 (w). MS (EI, 70 eV) m/z (%): 748 (26) $[M]^+$, 613 (5) $[M - Cp^*]^+$, 570 (32) $[M - bpy - Cl]^+$, 374 (100) $[Cp^*Ti(Cl)(bpy)]^+$, 218 (62) $[Cp^*Ti(Cl)]^+$, 156 (100) $[bpy]^+$, 135 (30) $[Cp^*]^+$. Anal. Calcd for $C_{40}H_{46}Cl_2N_4Ti_2$: C, 64.10; H, 6.19; N, 7.48. Found: C, 63.97; H, 6.01; N, 7.24.

Synthesis of $[\{Cp^*Ti(\mu\text{-Cl})(phen)\}_2]$ (4). Complex **4** was prepared in a fashion analogous to that of **3** but with phen (62.3 mg, 0.34 mmol) in place of bpy and with stirring in 40 mL of THF for 64 h, during which time the color of the suspension changed from orange to deep violet. Workup yielded a black solid in 89% yield (122.6 mg, 0.15 mmol), and single crystals of **4** suitable for X-ray diffraction were obtained from a saturated THF solution of complex after storage for several days at 4 °C. Mp: 145 °C (dec). IR (KBr; cm^{-1}): $\tilde{\nu}$ 2955 (m), 2888 (m), 2855 (s), 1560 (m), 1513 (m), 1464 (m), 1415 (s), 1378 (m), 1364 (m), 1293 (s), 1241 (m), 1221 (m), 1113 (m), 1088 (m), 1012 (w), 957 (s), 849 (s), 743 (s), 723 (s), 651 (w). MS (EI, 70 eV) m/z (%): 626 (15) $[M - Cp^* - Cl]^+$, 398 (100) $[Cp^*Ti(Cl)(phen)]^+$, 218 (20) $[Cp^*Ti(Cl)]^+$, 180 (98) $[phen]^+$, 135 (55) $[Cp^*]^+$. Anal. Calcd for $C_{44}H_{46}Cl_2N_4Ti_2$: C, 66.27; H, 5.81; N, 7.03. Found: C, 65.94; H, 5.78; N, 6.99.

Calculations. All DFT calculations were performed using version 3.0 of the ORCA software package.[14] The geometries of all complexes were optimized, in redundant internal coordinates without imposing geometric constraints, and all subsequent single-point calculations were performed at the B3LYP level of theory.[15] In all calculations, the def2-TZVP basis set was applied to Ti center, and all atoms coordinated to it, whereas the remaining C and H atoms were described by the slightly smaller def2-SV(P) basis sets.[16] Auxiliary basis sets, used to expand the electron density in the calculations, were chosen to match the orbital basis sets.[17] The RIJCOSX approximation

DOI: 10.1021/acs.inorgchem.5b00285
Inorg. Chem. 2015, 54, 4811−4820

was used to accelerate the calculations.[18] Reproduction of the crystallographically observed short Ti−Ti and bpy−bpy/phen−phen distances in the geometry optimized structures of **3** and **4** necessitated inclusion of dispersion forces via implementation of the D3ZERO empirical correction,[19] and for the sake of consistency this van der Waals correction was utilized throughout this study.

Throughout this study, our computational results are described using the broken symmetry (BS) approach.[20] The notation that follows is used to describe the BS solutions, where the given system is divided into two fragments. More specifically, the notation BS(m,n) refers to an open-shell BS state with m unpaired α-spin electrons localized on fragment 1 and n unpaired β-spin electrons localized on fragment 2. In this notation the standard high-spin, open-shell solution is written as BS($m + n$, 0). The BS(m, n) notation refers to the initial guess for the wave function, but the variational process has the freedom to converge to a solution of the form BS($m - n$, 0), in which the $n\beta$-spin electrons effectively pair up with ($n < m$)α-spin electrons on the partner fragment. Such a solution is then a standard $M_s \cong (m - n)/2$ spin-unrestricted or spin-restricted Kohn−Sham solution. As explained elsewhere,[21] the nature of the solution is investigated from corresponding orbital transformation (COT), which from the corresponding orbital overlaps displays whether the system should be described as a spin-coupled or a closed-shell solution. Orbitals and density plots were created using Chimera.[22]

RESULTS AND DISCUSSION

Synthesis of Complexes. From reaction of **1** with 1.5 equiv of magnesium metal and 2 equiv of (bpy^0) in THF, the moisture and air sensitive paramagnetic complex **2** was obtained as a black solid in 51% yield (eq 1).

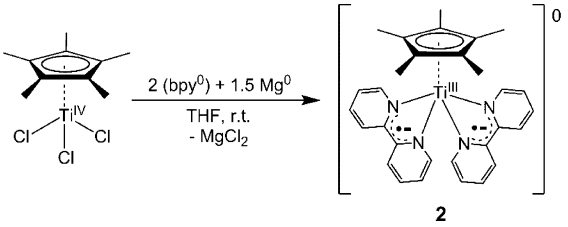

2 (1)

In contrast, reaction of **1** with only 1 equiv each of magnesium metal and (bpy^0) in THF yields the moisture and air sensitive black complex **3**, a dinuclear species containing a Ti(μ-Cl)$_2$Ti bridging moiety, in near quantitative yield (eq 2).

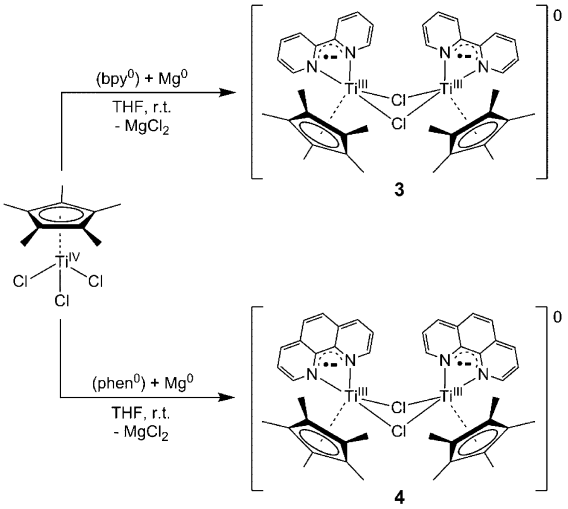

3 (2)

4 (3)

Performing this synthesis using 1 equiv of (phen^0) in place of (bpy^0) afforded the corresponding moisture and air sensitive black dinuclear complex **4** in 89% yield (eq 3).

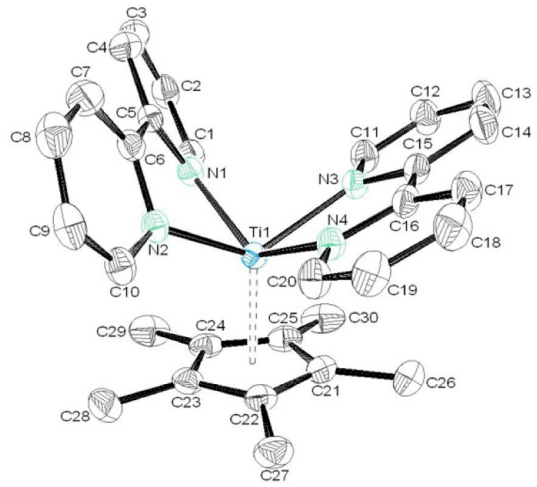

Figure 1. Molecular structure of complex **2** depicted with 50% probability thermal ellipsoids. Hydrogen atoms have been omitted for clarity.

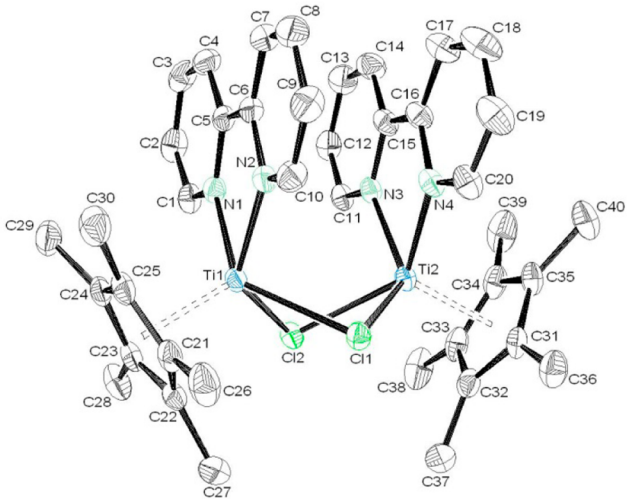

Figure 2. Molecular structure of complex **3** depicted with 50% probability thermal ellipsoids. Hydrogen atoms have been omitted for clarity.

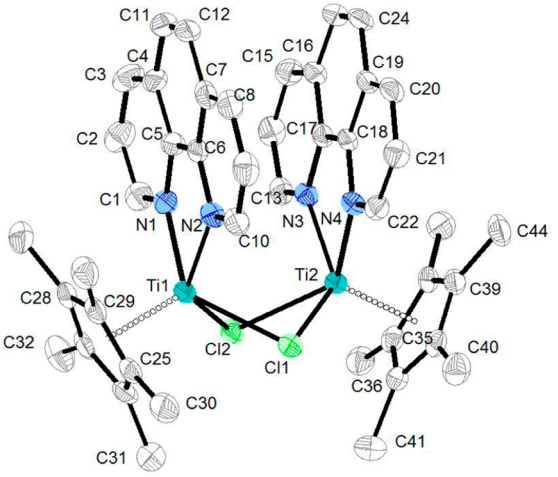

Figure 3. Molecular structure of complex **4** depicted with 50% probability thermal ellipsoids. Hydrogen atoms have been omitted for clarity.

Crystal Structures. The structures of **2**, **3**, and **4** have been determined at 153 K by high-resolution X-ray crystallography and are depicted in Figures 1, 2, and 3, respectively. The associated

DOI: 10.1021/acs.inorgchem.5b00285
Inorg. Chem. 2015, 54, 4811−4820

Table 1. Crystallographic Data for Complexes

	2	3	4
chem formula	$C_{30}H_{31}N_4Ti$	$C_{46}H_{60}Cl_2N_4Ti_2$	$C_{48}H_{54}Cl_2N_4OTi_2$
fw (g mol)	495.20	835.68	869.65
color	black	black	black
cryst syst	triclinic	orthorhombic	triclinic
space group	$P\bar{1}$	*Fdd*2	$P\bar{1}$
a (Å)	9.1011(18)	31.7878(13)	11.5694(9)
b (Å)	9.9158(18)	44.898(3)	11.7946(8)
c (Å)	15.331(3)	12.0946(6)	16.6783(13)
α (deg)	97.466(4)	90.00	100.756(9)
β (deg)	104.705(5)	90.00	106.971(8)
γ (deg)	107.848(5)	90.00	97.313(9)
V (Å^3)	1240.9(4)	17261.4(15)	2098.1(3)
Z	2	16	2
δ_{calcd} (g cm^{-3})	1.326	1.286	1.377
μ (mm^{-1})	0.371	0.530	0.550
λ (Å)	0.710 73	0.710 73	0.710 73
T (K)	153(2)	153(2)	153(2)
no. rflns collected	14 937	41 174	26 077
no. indep reflns *R*(int)	6310	8445	7773
no. reflns with $I > 2\sigma(I)$	4422	6747	3733
R_{int}	0.0407	0.0541	0.0852
F(000)	522	7072	912
R1 [$I > 2\sigma(I)$]	0.0445	0.0295	0.0349
wR2 (all data)	0.1059	0.0631	0.0669
params	321	489	524

crystallographic details are summarized in Table 1, and selected bond distances and angles are listed in Table 2.

In the mononuclear complex **2**, the Cp* monoanion is coordinated in an η^5-fashion, and the structural parameters of the two *N*,*N*′-coordinated bpy ligands are characteristic of π-radical anions.[1,3,4] More specifically, the bpy ligands display short $C_{py}-C_{py}$ bond lengths of 1.420(3) Å and long average intrachelate C−N distances of 1.388(3) Å, values that closely resemble those reported for the alkali metal salt of the $(bpy^{\bullet})^{1-}$ π-radical anion K(en)(bpy$^{\bullet}$) (1.431(3) and 1.389(3) Å, respectively; en = ethylene-1,2-diamine).[1] Interestingly, the angle between the planes defined by N−Ti−N at each bpy and the plane of the ligand itself are 12.2° and 22.4° for the first and second bpy ligand, respectively. Thus, the former Ti(bpy) moiety approaches planarity more than the latter. The aforementioned structural parameters point to an electronic structure $[(\eta^5\text{-Cp}^*)Ti^{III}(bpy^{\bullet})_2]^0$, a scenario in which the metal ion and two bpy ligands each possess a single unpaired electron.

The two titanium ions in neutral dinuclear complex **3** are connected by two bridging chloride ligands, and the $Ti(\mu\text{-Cl})_2Ti$ core displays a "butterfly" type structure (i.e., is nonplanar). All of the Cl−Ti−Cl and Ti−Cl−Ti angles, with average values of 77.4° and 83.3°, respectively, are significantly smaller than 90°. This is in contrast to $[\{(\eta^5\text{-Cp})_2Ti^{III}(\mu\text{-Cl})\}_2]^0$ (**6**),[11] which contains a planar $Ti(\mu\text{-Cl})_2Ti$ core and possesses Cl−Ti−Cl and Ti−Cl−Ti angles with average values of 77.98° and 101.96°, respectively. Accordingly, the intramolecular Ti···Ti distance in **3** of 3.3437(5) Å is significantly shorter than the Ti···Ti distance of ∼3.96 Å in **6**.[11] The geometrical details of the two *N*,*N*′-coordinated bpy ligands in **3** are again characteristic of $(bpy^{\bullet})^{1-}$ π-radical anions (see Table 2), and are suggestive of the electronic structure $[\{Cp^*Ti^{III}(\mu\text{-Cl})(bpy^{\bullet})\}_2]^0$.

Interestingly, the two $(bpy^{\bullet})^{1-}$ ligands in **3** are nearly coplanar, almost perfectly eclipsed, and the distances between

Table 2. Selected Bond Distances (Å) and Angles (deg) from the Crystal Structures of the Complexes

	Complex **2**		
Ti−N(1)	2.116(2)	N(1)−C(5)	1.393(3)
Ti−N(2)	2.110(2)	C(5)−C(6)	1.420(3)
Ti−N(3)	2.178(2)	N(2)−C(6)	1.390(3)
Ti−N(4)	2.193(2)	N(3)−C(15)	1.387(2)
		C(15)−C(16)	1.420(3)
		N(4)−C(16)	1.383(3)
	Complex **3**		
Ti(1)−N(1)	2.135(2)	N(1)−C(5)	1.385(3)
Ti(1)−N(2)	2.137(2)	C(5)−C(6)	1.429(4)
Ti(2)−N(3)	2.134(2)	N(2)−C(6)	1.389(3)
Ti(2)−N(4)	2.136(2)	N(3)−C(15)	1.381(3)
Ti(1)−Cl(1)	2.527(1)	C(15)−C(16)	1.432(4)
Ti(1)−Cl(2)	2.513(1)	N(4)−C(16)	1.387(3)
Ti(2)−Cl(1)	2.514(1)		
Ti(2)−Cl(2)	2.507(1)		
Ti(1)···Ti(2)	3.344(1)		
Cl(1)−Ti(2)−Cl(2)	77.61(1)		
Ti(2)−Cl(1)−Ti(1)	83.11(2)		
Cl(1)−Ti(1)−Cl(2)	77.26(1)		
Ti(1)−Cl(2)−Ti(2)	83.53(2)		
	Complex **4**		
Ti(1)−N(1)	2.131(2)	N(1)−C(5)	1.383(5)
Ti(1)−N(2)	2.159(3)	C(5)−C(6)	1.398(4)
Ti(2)−N(3)	2.161(2)	N(2)−C(6)	1.392(4)
Ti(2)−N(4)	2.142(3)	N(3)−C(17)	1.377(5)
Ti(1)−Cl(1)	2.496(1)	C(17)−C(18)	1.409(4)
Ti(1)−Cl(2)	2.519(1)	N(4)−C(18)	1.383(3)
Ti(2)−Cl(1)	2.518(1)		
Ti(2)−Cl(2)	2.506(1)		
Ti(1)···Ti(2)	3.304(1)		
Ti(1)−Cl(1)−Ti(2)	82.43(3)		
Ti(1)−Cl(2)−Ti(2)	82.23(3)		
Cl(1)−Ti(2)−Cl(2)	78.20(3)		
Cl(1)−Ti(1)−Cl(2)	78.38(3)		

the centroids of the pyridine rings facing one another are only 3.2557(1) and 3.3272(1) Å, which are shorter than the Ti···Ti distance and the van der Waals radii of their constituent atoms. These structural features are typical of π-stacked dimers of planar organic radicals,[23] wherein the singly occupied molecular orbitals (SOMOs) directly overlap with one another to form multicentered two-electron bonds known as "pancake bonds".[24] This typically results in diamagnetism at or below room temperature. Indeed, the observed diamagnetic ground state of the previously reported scandium complex $[\{(\eta^5\text{-Cp}^*)Sc^{III}(\mu\text{-Cl})(bpy^{\bullet})\}_2]^0$ (**7**),[12] which is structurally analogous to **3**, was calculated to originate from this phenomenon.[4a]

With the exception of *N*,*N*′-coordinated phen ligands coordinating in place of bpy, the structure of $[\{(\eta^5\text{-Cp}^*)Ti(\mu\text{-Cl})(phen)\}_2]^0$ (**4**) is qualitatively identical to that of complex **3**. More specifically, the geometrical features of the butterfly type $Ti(\mu\text{-Cl})_2Ti$ core in **4** are very similar to those in **3**, and a strong intramolecular π-stacking interaction is observed between the two eclipsed, effectively coplanar phen ligands. Furthermore, the $C_{py}-C_{py}$ and intrachelate C−N bond lengths in the phen ligands are significantly shorter and longer, respectively, than those in *N*,*N*′-coordinated neutral $(phen^0)$ ligands. As we will show later, in close analogy with bpy, the $C_{py}-C_{py}$ and intrachelate C−N bond distances in phen reflect the

DOI: 10.1021/acs.inorgchem.5b00285
Inorg. Chem. 2015, 54, 4811−4820

oxidation level of the ligand, and those in complex **4** are indicative of $(phen^{\bullet})^{1-}$. In summary, the geometrical features of **4** signify that it possesses the electronic structure $[\{(\eta^5\text{-Cp}^*)\text{-}Ti^{III}(\mu\text{-Cl})(phen^{\bullet})\}_2]^0$, which is analogous to that of **3**.

Electronic Spectra and Magnetism. Electronic spectra (300−1600 nm) of complexes **2**, **3**, and **4** (Figure 4), recorded

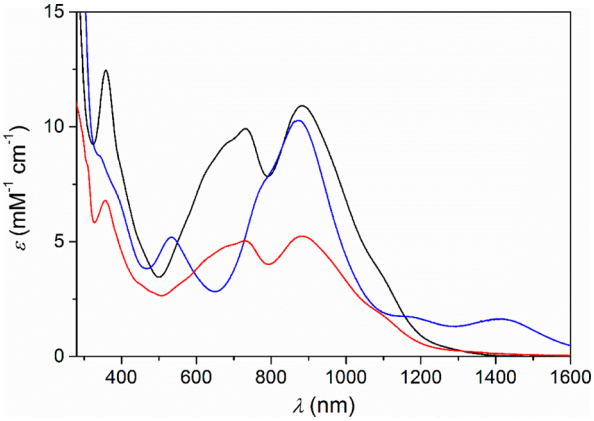

Figure 4. Electronic spectra of complexes **2** (red), **3** (black), and **4** (blue), recorded in toluene solution at room temperature.

at room temperature in toluene solution under anaerobic conditions, all display intense absorption bands ($\varepsilon > 3 \times 10^3$ M^{-1} cm^{-1}) in the visible and near-infrared regions. The spectra of **2** and **3** are nearly identical in form, and both display intense bands at 1100 (sh), 890, 720, 680 (sh), and ∼400 nm that are associated with $\pi \rightarrow \pi^*$ transitions of *N*,*N*′-coordinated $(bpy^{\bullet})^{1-}$ π-radical anions.[25] Examples include those in the spectrum of the homoleptic complex $[Ti^{III}(^{Me}bpy^{\bullet})_3]^0$ (^{Me}bpy = 4,4′-dimethyl-2,2′-bipyridine), which contains three $(bpy^{\bullet})^{1-}$ ligands.[25,26] Similarly, the spectrum of **4** closely resembles that of $[Ti^{III}(^{Me}phen^{\bullet})_3]^0$,[27] and displays transitions (ε, M^{-1} cm^{-1}) typical of the $(phen^{\bullet})^{1-}$ π-radical anion at 1400 (1.2×10^3), 1200 (1.2×10^3), 870 (1.1×10^4), 780 (sh), 540 (5×10^3), 390 (sh), and 350 (8×10^3) nm. Crucially, the UV−vis spectra of **2**, **3**, and **4** exclude descriptions of their electronic structures as $[(\eta^5\text{-Cp}^*)Ti^{I}(bpy^0)_2]^0$, $[\{(\eta^5\text{-Cp}^*)Ti^{II}(\mu\text{-Cl})(bpy^0)\}_2]^0$, and $[\{(\eta^5\text{-Cp}^*)Ti^{II}(\mu\text{-Cl})(phen^0)\}_2]^0$.

Magnetic susceptibility data for solid samples of **2**, **3**, and **4** were recorded using a SQUID magnetometer at a field of 1.0 T, in the temperature range 3−300 K. The resulting temperature dependence of the magnetic moments of **2** and **3** are shown in Figure 5, that of **4** is given in Supporting Information Figure S1, and the parameters used to simulate the data of all complexes are given in Supporting Information Table S1. The temperature independent magnetic moment of 1.74 μ_B measured for **2** indicates that it possesses an $S = {}^1/_2$ ground state; precedent would suggest this would arise from strong intramolecular antiferromagnetic coupling ($J_{exp} < -400$ cm^{-1}) between the unpaired spin on the Ti ion and that on one of the constituent $(bpy^{\bullet})^{1-}$ ligands in the postulated $[(\eta^5\text{-Cp}^*)Ti^{III}(bpy^{\bullet})_2]^0$ electronic structure. The residual unpaired electron would then be expected to reside predominantly in a π^*-orbital of (bpy^0). The magnetic moment of the dinuclear complex **3** was found to increase monotonically from 2.55 μ_B at 300 K to 2.81 μ_B at 5 K, which indicates that it possesses a triplet ($S = 1$) ground state. (Similar results were found for **4**.) We successfully modeled this behavior using the spin-Hamiltonian $\hat{H} = -2JS_1 \cdot S_2$, with $S_1 = S_2 = {}^1/_2$, $g = 1.98$, and a moderately

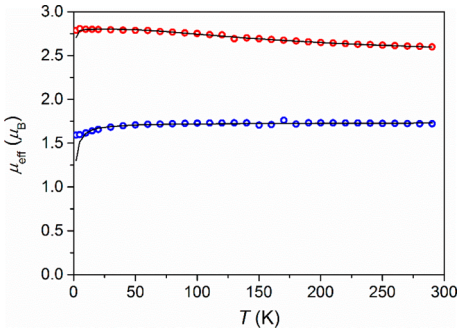

Figure 5. Plots of magnetic moment, μ_{eff}, versus temperature for solid samples of **2** (blue circles) and **3**·$(THF)_{4.5}$ (red circles). The solid lines are simulations created using the parameters listed in Table S1 in the Supporting Information.

strong ferromagnetic coupling constant J_{expt} of +72 cm^{-1} (for complex **4**, $g = 2.00$ and $J_{expt} = +70$ cm^{-1}). This coupling is weak relative to that observed in most other Ti^{III} complexes. For instance, a $J_{expt} = +83$ cm^{-1} has been reported for $[\{Cp_2Ti^{III}\}_2(\mu\text{-O})]^0$,[28] in which a linear $Ti^{III}-O-Ti^{III}$ arrangement excludes the possibility of a direct Ti···Ti interaction.

Calculations. The electronic structures of complexes **2**, **3**, and **4** have been investigated with density functional theory (DFT), using both geometry optimization and single-point calculations utilizing X-ray crystallographic atomic coordinates (see Experimental Section for further details). The results obtained in both cases are qualitatively identical, and throughout this study we focus on the former. Other than a slight overestimation of the titanium−ligand donor atom bond lengths by up to 0.05 Å, which is typically observed for the B3LYP functional, the agreement between the calculated and experimental structures was found to be excellent. Calculations were performed using the broken symmetry BS(*m*, *n*) methodology[20] (see the Experimental Section for further details) and magnetic coupling constants obtained via the Yamaguchi approach (eq 4).[29] A detailed description of the meaning of the spin expectation values $\langle S^2 \rangle$ and the energies E_{HS} and E_{BS} have been described elsewhere.[29]

$$J_{calcd} = -\frac{E_{HS} - E_{BS}}{\langle S^2 \rangle_{HS} - \langle S^2 \rangle_{BS}} \quad (4)$$

In order to calibrate our methodology, we first calculated the molecular and electronic structure of the well-characterized dinuclear complex **6**,[11,31] which is experimentally known to possess singlet ground and triplet excited states, related by a magnetic coupling constant (J_{expt}) of −111 cm^{-1}.[11] The geometry optimized BS(1, 1) state was found to be 23 kcal mol^{-1} lower in energy than the corresponding closed-shell ($S = 0$) restricted Kohn−Shan (RKS) solution (Supporting Information Table S2). The structural parameters of the former are in excellent agreement with experimental results (Supporting Information Table S9), as is the antiferromagnetic coupling constant (J_{calcd}) of −95 cm^{-1} obtained from a single-point calculation utilizing its atomic coordinates (Table 3), which indicates that the BS(1,1) solution is the ground state. The Mulliken spin density population analyses and qualitative frontier molecular orbital (FMO) diagrams for both the ground state and $S = 1$ excited state solutions (Supporting Information Figures S2, S14, and S15) confirm that each Ti ion possesses a d^1 electron configuration.

Consistent with published Hartree−Fock−Slater quantum chemical studies,[31] we obtained SOMOs in both the BS(1, 1)

DOI: 10.1021/acs.inorgchem.5b00285
Inorg. Chem. 2015, 54, 4811−4820

Table 3. Magnetic Properties of Selected Mononuclear and Dinuclear Titanium Complexes

complex	J_{expt} (cm^{-1})[a]	J_{calcd} (cm^{-1})[a]	ground state (S)	ref
	Mononuclear			
$[Ti^{III}(bpy^{\bullet})_3]^0$	very strong af	n.a.	0	26
$[Ti^{III}(bpy^{\bullet})_2(bpy^0)]^{1+}$	n.a.	−693	$^1/_2$	4e
$[(\eta^5\text{-Cp})_2Ti^{III}(bpy^{\bullet})]^0$ [b]	−300	−150	0	4a, 5a
$[(\eta^5\text{-Me}_4\text{Cp})_2Ti^{III}(bpy^{\bullet})]^0$ [b]	n.a.	n.a.	0	6a
$[(\eta^5\text{-Cp*})_2Ti^{III}(bpy^{\bullet})]^0$ [b]	n.a.	n.a.	1	6a
2	very strong af	−806	$^1/_2$	this work
$[(\eta^5\text{-Cp*})Ti^{III}(bpy^{\bullet})Cl]^0$ [c]	n.a.	+396	1	this work
$[(\eta^5\text{-Cp*})Ti^{III}(bpy^{\bullet})Cl_2]^{1-}$ [c]	n.a.	+165	1	this work
	Dinuclear			
6	−111	−95	0	11, this work
$[\{(\eta^5\text{-Cp})(^t\text{Bu}_3\text{PN})Ti^{III}Cl\}_2]^0$	n.a.	−419	0	30, this work
3	+72	+46	1	this work
4	+70	+59	1	this work

[a]Experimentally observed (expt) and calculated (calcd) magnetic coupling constants J in cm^{-1} obtained using the spin-Hamiltonian $\hat{H} = -2J\sum_i S_{Ti}\cdot S_i$ [$S_i = {}^1/_2$; i = 1, 2, 3 (the number of unpaired electrons on the ligands); S_{Ti} (local spin at the Ti ion) = $^1/_2$]; n.a. = not available. Calculated values obtained using geometry optimized structures. [b]Ground state from temperature dependence of the intensity of the triplet EPR signal. [c]Hypothetical species.

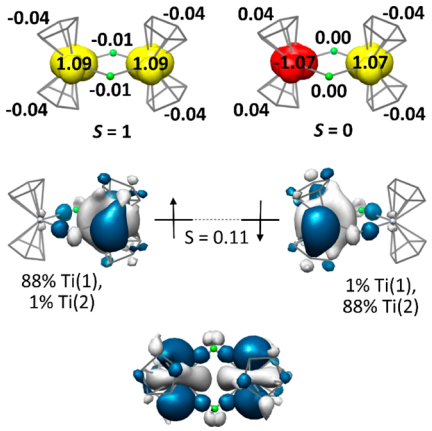

Figure 6. Top: Mulliken spin density plots (yellow, α-spin; red, β-spin), plus spin density populations, calculated for the S = 1 UKS (left) and S = 0 BS(1, 1) (right) geometry optimized structures of $[\{(Cp)_2Ti(\mu\text{-Cl})\}_2]^0$. Bottom: SOMOs of the S = 0 BS(1, 1) geometry optimized structure of $[\{(Cp)_2Ti(\mu\text{-Cl})\}_2]^0$ plotted separately (above) and together (below). Rendered using an isosurface contour value of 0.02.

and S = 1 solutions that lie perpendicular to the Ti···Ti axis and are primarily d_{z^2} in character (Figure 6 and Supporting Information Figure S15). On the basis of the qualitative FMO diagram for the S = 1 solution (Supporting Information Figure S15), it would appear that the SOMOs comprise a bonding and antibonding pair. As a consequence of the orientation of the d_{z^2} orbitals, there is minimal interaction with the chloride bridging ligands, and the bonding interaction that gives rise to the diamagnetic ground state of **6** appears, therefore, to derive from direct overlap of the aforementioned Ti d-orbitals. The long intramolecular Ti···Ti distance of 3.95 Å combined with the contracted nature of the Ti orbitals results in this interaction being very weak (overlap integral S = 0.11). Note that it is clear that this interaction does not equate to a Ti−Ti bond. These conclusions are in agreement with those arrived at by Stucky et al.[11] and the quantum chemical studies referred to above.[31] Consistent with this model, the fluoride-, bromide-, and iodide-bridged analogues of **6**, which all have a planar $Ti(\mu\text{-X})_2Ti$ bridging unit with a long Ti···Ti distance, all possess S = 0 ground states.[10] This can be interpreted as suggesting that the identity of the bridging group is not a critically important component of the magnetic interaction.

In an effort to try to establish the validity of the direct Ti···Ti d-orbital overlap model, a dinuclear complex was sought that is similar in nature to **6** but possesses a significantly shorter intramolecular Ti···Ti distance. To this end, calculations were performed for $[\{(\eta^5\text{-Cp*})(^t\text{Bu}_3\text{PN})Ti^{III}(\mu\text{-Cl})\}_2]^0$, for which brief Extended Hückel MO calculations, an X-ray crystal structure, and a single crystal EPR study at ambient temperature have previously been reported.[30] The geometry optimized structure of this complex was found to display excellent agreement with experiment (Supporting Information Table S15), with a planar $Ti(\mu\text{-Cl})_2Ti$ ring and a relatively short Ti···Ti distance of 3.666 Å. Its ground state was found to be an open-shell BS(1,1) singlet state (Supporting Information Table S8), wherein the two Ti-centered unpaired spins couple strongly in an antiferromagnetic fashion (J_{calcd} = −419 cm^{-1}). As was the case for **6**, the SOMOs of the S = 1 excited state comprise a metal-centered bonding and antibonding combination that are primarily d_{z^2} in character, and are oriented perpendicular to the Ti···Ti axis (Supporting Information Figure S28). From examination of its qualitative FMO diagrams (Supporting Information Figures S27 and S28), it is apparent that a direct Ti···Ti interaction is operative in this case (overlap integral S = 0.19). This discernible difference from **6** derives from the shorter Ti···Ti distance in $[\{(\eta^5\text{-Cp*})(^t\text{Bu}_3\text{PN})Ti^{III}(\mu\text{-Cl})\}_2]^0$, and is the origin of the larger J_{calcd} value and overlap integral in the latter complex.

In the case of the mononuclear complex **2**, unrestricted Kohn−Sham (UKS) calculations for the experimentally observed $S = {}^1/_2$ ground state converged to a BS(2, 1) solution that is 5.4 kcal mol^{-1} lower in energy than the $S = {}^3/_2$ excited state (Supporting Information Table S3). Magnetic coupling constants, J_{cacld}'s, of −1122 and −806 cm^{-1} were obtained from single-point calculations using atomic coordinates of the X-ray and the BS(2, 1) geometry optimized structures, respectively. These values correspond to very strong antiferromagnetic coupling and are consistent with the temperature independent μ_{eff} of 1.73 μ_{BM} measured for this complex in the temperature range 10−300 K. Agreement between the calculated and experimental structures was found to be excellent (Supporting Information Table S10). Examples include the calculated C_{py}−C_{py} bond distances of 1.427 and 1.433 Å and that observed experimentally of 1.420(3) Å. These values agree nicely with the corresponding bond distance of 1.431(3) Å in the salt $K(en)(bpy^{\bullet})^1$ and the average value C_{py}−C_{py} bond length of 1.431(6) Å in $[Ti^{III}(Mebpy^{\bullet})_3]^0$,[26] and are indicative of the $(bpy^{\bullet})^{1-}$ ligand redox state.

Consistent with the structural parameters of **2**, the Mulliken spin density population analyses for both the $S = {}^1/_2$ and $^3/_2$ states (Figure 7) clearly show that one unpaired electron resides on the Ti center and on each of the bpy ligands, which corresponds to the electronic structure $[(\eta^5\text{-Cp*})Ti^{III}(bpy^{\bullet})_2]^0$. However, the qualitative FMO diagram for the doublet ground state provides a much less clear-cut picture, with both α-spin orbitals displaying significant Ti character (Figure 7). More specifically, the unpaired electron and that involved in antiferromagnetic coupling reside in SOMOs with 57% and 46% Ti character, respectively, with the major contributor in both cases being the $d_{x^2-y^2}$ orbital (>30%) and the non-Ti balance being

DOI: 10.1021/acs.inorgchem.5b00285
Inorg. Chem. 2015, 54, 4811−4820

primarily derived from the same bpy ligand. This extensive mixing of the α-spin orbitals arises from significant covalency, and is also evident in the large overlap integral of 0.60 associated with the antiferromagnetic interaction depicted in Figure 7. As a consequence, it is difficult to assign either of the

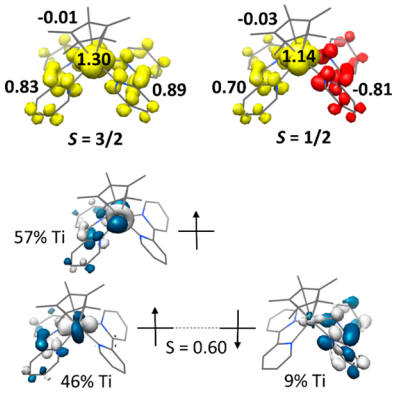

Figure 7. Top: Mulliken spin density plots (yellow, α-spin; red, β-spin), plus spin density populations, calculated for the $S = {}^3/_2$ UKS (left) and $S = {}^1/_2$ BS(2, 1) (right) geometry optimized structures of **2**. Bottom: Qualitative frontier molecular orbital diagram of **2** obtained using its $S = {}^1/_2$ BS(2, 1) geometry optimized structure (isosurface contour value = 0.05).

α-spin SOMOs as being truly metal- or ligand-based, and stating that the $[(\eta^5\text{-Cp*})\text{Ti}^{\text{III}}(\text{bpy}^{\bullet})_2]^0$ ($S = {}^1/_2$) ground state is obtained either by antiferromagnetic coupling of the two ligand radicals or by the Ti^{III} ion with a ligand radical would not be strictly correct in either case.

As shown by X-ray crystallography, the structure of dinuclear **3** (Figure 3) is nearly identical to that of its scandium analogue $[\{(\eta^5\text{-Cp*})\text{Sc}^{\text{III}}(\mu\text{-Cl})(\text{bpy}^{\bullet})\}_2]^0$ (**7**),[4a] but in contrast to the diamagnetism of the latter, the former exhibits an $S = 1$ ground state. Geometry optimization for **3** reproduced this observation by yielding a triplet state 26.1 and 6.2 kcal mol^{-1} lower in energy than the closed-shell $S = 0$ and $S = 2$ solutions, respectively (Supporting Information Table S4). Furthermore, BS(1, 1) single-point calculations using the atomic coordinates of the X-ray structure and the BS(1, 1) geometry optimized structure provided J_{calcd} values of +86 and +46 cm^{-1}, respectively, which are in excellent agreement with the experimental value of +70 cm^{-1}. The structural parameters of the geometry optimized structure of the $S = 1$ state closely resemble those of the X-ray structure of **3** (Supporting Information Table S11) with average $C_{\text{py}}-C_{\text{py}}$ bond distances of 1.440 Å, characteristic of $(\text{bpy}^{\bullet})^{1-}$ ligands, a relatively short Ti···Ti distance of 3.34 Å, and centroid−centroid separations between eclipsed pyridine rings of 3.273 and 3.292 Å.

As observed in calculations for **7**, the close proximity of the two near parallel $(\text{bpy}^{\bullet})^{1-}$ ligands combined with their eclipsed orientation allows for a direct overlap of their SOMOs and formation of a pancake bond, in which the bonding combination is doubly occupied (Figure 8). This leaves two unpaired electrons, one on each Ti ion, which couple ferromagnetically to yield the observed triplet ground state. This occurs despite the relatively short intramolecular Ti···Ti distance in **3**, which based upon our calculations for **6** and $[\{(\eta^5\text{-Cp*})(^t\text{Bu}_3\text{PN})\text{Ti}^{\text{III}}(\mu\text{-Cl})\}_2]^0$ might be expected to lead to enhanced overlap of the metal-based SOMOs. However, the puckered nature of the $\text{Ti}(\mu\text{-Cl})_2\text{Ti}$ bridging unit in **3** causes the two SOMOs to be

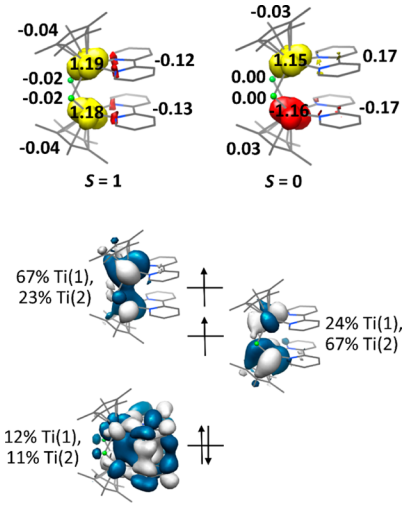

Figure 8. Top: Mulliken spin density plots (yellow, α-spin; red, β-spin), plus spin density populations, calculated for the $S = 1$ UKS (left) and $S = 0$ BS(1, 1) (right) geometry optimized structures of **3**. Bottom: Qualitative FMO diagram for the $S = 1$ geometry optimized structure of **3** (isosurface contour value = 0.02).

canted relative to one another, which reduces the overall efficiency of the metal−metal bonding interaction, while also increasing the degree of orbital overlap with the chloride bridging ligands. Indeed, in contrast with the $S = 1$ excited states of **6** and $[\{(\eta^5\text{-Cp*})(^t\text{Bu}_3\text{PN})\text{Ti}^{\text{III}}(\mu\text{-Cl})\}_2]^0$, it is clear that the two SOMOs of **3** do not comprise a bonding/antibonding pair. As a consequence, the superexchange interaction prevails, and ferromagnetic coupling is observed. As previously mentioned, it is likely that the "butterfly" type geometry of the $\text{Ti}(\mu\text{-Cl})_2\text{Ti}$ bridging unit is primarily due to the strong pancake bonding interaction in the bridging diamagnetic $\{(\text{bpy})_2\}^{2-}$ unit. In other words, the π-stacking interaction determines the ground state of the complex.

Geometry optimization of the BS(1,1) open-shell singlet excited state of **3** yielded a structure virtually identical to that of the triplet ground state (Supporting Information Table S11), and consistent with retention of the pancake bond between the two cofacial $(\text{bpy}^{\bullet})^{1-}$ ligands. This result is in good agreement with the conclusion that the ground triplet and excited singlet states of **3** differ only with respect to the spin orientation of the magnetic orbitals on the central Ti ions, with them ferromagnetically coupling in the former case and antiferromagnetically in the latter case (Figure 8). This does not perturb the Ti···Ti separation significantly (3.36 and 3.34 Å in the $S = 0$ and 1 solutions, respectively) due to the lack of significant direct metal−metal bonding, despite its relatively short distance.

In contrast, the geometry optimized structure of the $S = 2$ excited state of **3** displays significant geometric differences when compared to the structure of its $S = 1$ ground state (Supporting Information Figure S11). More specifically, the average separation between the centroids of the eclipsed pyridine rings and the Ti···Ti distance increases to 3.70 and 3.50 Å, respectively, and the bpy ligands move into a staggered arrangement, with the ($C_{\text{py}}-C_{\text{py}}$ centroid)−Ti−Ti−($C_{\text{py}}-C_{\text{py}}$ centroid) dihedral angle increasing from 2.4° in the $S = 1$ solution to 13.2° in the $S = 2$ solution. This derives from disruption of the pancake bond, and it causes the two unpaired spins on the resulting $(\text{bpy}^{\bullet})^{1-}$ ligands to couple ferromagnetically with those on the two Ti^{III} ions (Supporting Information

DOI: 10.1021/acs.inorgchem.5b00285
Inorg. Chem. 2015, 54, 4811−4820

Tables S6 and S20). This model for the exchange pathway implies that spin coupling between the central Ti^{III} ion and its *N*,*N*′-coordinated $(bpy^{\bullet})^{1-}$ π-radical anion, whether ferro- or antiferromagnetic, must be very weak relative to the very strong interaction between the $(bpy^{\bullet})^{1-}$ ligands in the $\{(bpy)_2\}^{2-}$ unit. In order to test this model we have performed geometry optimizations and single-point calculations using atomic coordinates derived from a truncation of the X-ray structure of **3** for the hypothetical molecules $[(\eta^5\text{-Cp*})Ti^{III}(bpy^{\bullet})Cl]^0$ and $[(\eta^5\text{-Cp*})Ti^{III}(bpy^{\bullet})Cl_2]^{1-}$.

For the monomeric complex $[(\eta^5\text{-Cp*})Ti^{III}(bpy^{\bullet})Cl]^0$ geometry optimization yielded an $S = 1$ ground state that was calculated to be 1.3 and 9.1 kcal mol^{-1} lower in energy than the corresponding open-shell BS(1,1) closed-shell RKS singlet solutions (Supporting Information Table S6). The structural parameters of the triplet solution are very similar to the corresponding component of the X-ray structure of **3** (Supporting Information Table S3). Most pertinently, the former possesses a $C_{py}-C_{py}$ bond length (1.436 Å) characteristic of a $(bpy^{\bullet})^{1-}$ π-radical anion, which renders the central Ti ion trivalent (d^1). This inference is confirmed by the spin density plots and qualitative FMO diagram depicted in Figure 9.

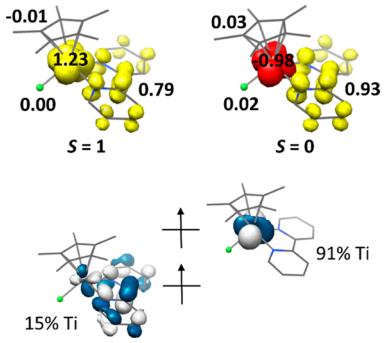

Figure 9. Top: Mulliken spin density plots (yellow, α-spin; red, β-spin), plus spin density populations, calculated for the $S = 1$ UKS (left) and $S = 0$ BS(1, 1) (right) geometry optimized structures of $[(\eta^5\text{-Cp*})Ti^{III}(bpy^{\bullet})Cl]^0$. Bottom: Qualitative frontier molecular orbital diagram of $[(\eta^5\text{-Cp*})Ti^{III}(bpy^{\bullet})Cl]^0$ obtained using its $S = 1$ geometry optimized structure (isosurface contour value = 0.05).

Yamaguchi coupling constants of +396 and +593 cm^{-1} were calculated using the BS(1,1) optimized geometry and atomic coordinates taken from the X-ray structure, respectively, which are indicative of strong ferromagnetic coupling.

Geometry optimization for the monoanion $[(\eta^5\text{-Cp*})Ti^{III}(bpy^{\bullet})Cl_2]^{1-}$ also revealed a triplet ground state and a diradical singlet excited state (Supporting Information Table S5), both of which display $C_{py}-C_{py}$ bond lengths (1.430 and 1.428 Å, respectively) very similar to those seen in the X-ray structure of **3** and characteristic of $(bpy^{\bullet})^{1-}$ (Supporting Information Table S12). Additionally, the Mulliken spin density plots calculated using the experimental atomic coordinates and those of the geometry optimized structure, which can be found in Supporting Information Figures S7 and S8, are nearly identical and reaffirm the general similarity of the two sets of structures. A single-point calculation performed using the atomic coordinates of the BS(1, 1) geometry optimized structure yielded a value of $J_{calcd} = +165$ cm^{-1}. This value is indicative of a strong ferromagnetic coupling between the respective unpaired spins of the $(bpy^{\bullet})^{1-}$ ligand and the Ti^{III} ion. In contrast, when using atomic coordinates taken from the X-ray structure of **3** the BS(1,1) solution was found to be at an energy nearly identical to that of the triplet state, and a $J_{calcd} = -26$ cm^{-1} was obtained, which equates to very weak antiferromagnetic coupling.

The ferromagnetic coupling constants calculated for the theoretical molecules $[(\eta^5\text{-Cp*})Ti^{III}(bpy^{\bullet})Cl]^0$ and $[(\eta^5\text{-Cp*})Ti^{III}(bpy^{\bullet})Cl_2]^{1-}$ are in sharp contrast to the strong antiferromagnetic coupling observed and calculated for closely related complexes **2** and $[(\eta^5\text{-Cp*})_2Ti^{III}(bpy^{\bullet})]^0$ ($J_{obs} = -300$ cm^{-1} and $J_{calc} = -150$ cm^{-1}).[4b] The origin of this discrepancy lies in the greater strength of Ti−Cl bonding relative to $Ti-N_{bpy}$ bonding, which leads to preferential orientation of the coordinate axis to accommodate both σ- and π-bonds of the former type. This is clearly discernible in the unoccupied metal-centered antibonding FMOs of $[(\eta^5\text{-Cp*})Ti^{III}(bpy^{\bullet})Cl]^0$ and $[(\eta^5\text{-Cp*})Ti^{III}(bpy^{\bullet})Cl_2]^{1-}$ depicted in Supporting Information Figures S21 and S22. The upshot of this is that the essentially nonbonding metal-centered SOMOs in these complexes lie close to the plane of their respective bpy ligands, which is orthogonal to the π^* orbitals of bpy. Hence, the magnetic interaction between the metal and ligand-centered unpaired spins is ferromagnetic.

In the case of complex **2**, other than bonding to the Cp* ring, the Ti d-orbitals only have to accommodate interactions with the orbitals of bpy (Supporting Information Figure S16). As a consequence, its metal-centered SOMO does not lie in the plane of the bpy ligand, which means that it is not orthogonal to their π^* orbitals, and antiferromagnetic coupling is observed. Interestingly, the $Ti-N_{bpy}$ bonding interactions in **2** are accentuated by, and are likely the cause of, the experimentally observed and computationally reproduced distortion of the plane of the bpy ligands from the N−Ti−N plane associated with their coordination (see earlier).

The DFT calculations for these hypothetical molecules bolster the conclusion that the spin coupling pathway in **3** does not involve strong antiferromagnetic coupling between the unpaired spin of the Ti^{III} ion and their $(bpy^{\bullet})^{1-}$ ligands. Rather, formation of a multicentered two-electron bond between the SOMOs of the two $(bpy^{\bullet})^{1-}$ anions results in formation of a doubly occupied molecular orbital. In essence, this is an $S = 0$ $\{(bpy)_2\}^{2-}$ bridging unit. Ferromagnetic coupling of the two Ti-centered unpaired spins yields the experimentally observed triplet ground state (Figure 8).

Lastly, calculations for complex **4** were conducted in the same manner as those for **3**, and analogous results were obtained (see Supporting Information). The geometry optimized structure of **4** is in very good agreement with the corresponding X-ray structure (Supporting Information Table S14), with two eclipsed cofacially $\pi-\pi$ stacked phen ligands, which possess $C_{py}-C_{py}$ bond lengths characteristic of $(phen^{\bullet})^{1-}$ π-radical anions; a buttefly type $Ti(\mu\text{-Cl})_2Ti$ core, which has a relatively short Ti···Ti separation of 3.311 Å; and phen−phen separations of approximately 3.3 Å. These structural features are characteristic of direct overlap of the two $(phen^{\bullet})^{1-}$ SOMOs to form a pancake bond, which affords a diamagnetic $\{(phen)_2\}^{2-}$ bridging unit and leaves the two Ti-centered unpaired spins to couple in a ferromagnetic fashion ($J_{calcd} = +59$ and +69 cm^{-1} obtained using the BS(1, 1) geometry optimized and X-ray structural atomic coordinates, respectively) to yield the experimentally observed triplet ground state (Supporting Information Figures S11, S12, and S24).

CONCLUSION

The most salient features of new complexes **2**, **3** and **4** are summarized in the following paragraphs.

DOI: 10.1021/acs.inorgchem.5b00285
Inorg. Chem. 2015, 54, 4811−4820

All species, mononuclear **2**, and dinuclear **3** and **4**, contain η^5-coordinated pentamethylcyclopentadienyl (Cp*) anions and *N*,*N*′-coordinated $(bpy^{\bullet})^{1-}$ or $(phen^{\bullet})^{1-}$ π-radical ligands. The $(bpy^{\bullet})^{1-}$ oxidation level was identified crystallographically using its $C_{py}-C_{py}$ and intrachelate $C_{py}-N$ bond lengths, which are significantly shorter and longer, respectively, than those in neutral (bpy^0) ligands. Furthermore, all black compounds exhibit very intense bands in the visible and near-infrared regions that are characteristically associated with $\pi \rightarrow \pi^*$ transitions in $(bpy^{\bullet})^{1-}/(phen^{\bullet})^{1-}$ π-radicals. As a consequence, it can be concluded that **2**, **3**, and **4** all contain a central Ti^{III} ion possessing a d^1 electronic configuration. In all cases, the structural parameters of the optimized geometries were found to display excellent agreement with experiment.

Mononuclear complex **2** carries three unpaired electrons, one on the Ti^{III} ion and one on each of the two $(bpy^{\bullet})^{1-}$ ligands, which strongly antiferromagnetically couple to yield an $S = {}^1/_2$ ground state. Taken as a whole, DFT calculations support this $[(\eta^5\text{-Cp}^*)Ti^{III}(bpy^{\bullet})_2]^0$ electronic structure picture. From this perspective, it is somewhat surprising that the coupling in hypothetical complexes $[(\eta^5\text{-Cp}^*)Ti^{III}(bpy^{\bullet})Cl]^0$ and $[(\eta^5\text{-Cp}^*)Ti^{III}(bpy^{\bullet})Cl_2]^{1-}$ has been calculated to be ferromagnetic. This quite simply stems from reorientation of the d-orbitals to accommodate the strong σ- and π-bonding interactions with the chloride ligands, which renders the metal-centered SOMO orthogonal to singly occupied π^* orbitals of the $(bpy^{\bullet})^{1-}$ ligands.

In dinuclear complexes **3** and **4** direct intramolecular overlap of the SOMOs of the two coplanar and cofacial $(bpy^{\bullet})^{1-}$ or $(phen^{\bullet})^{1-}$ ligands affords diamagnetic $\{(bpy)_2\}^{2-}$ and $\{(phen)_2\}^{2-}$ bridging units. The residual Ti-centered unpaired spins in the resulting bent $Ti(\mu\text{-Cl})_2Ti$ cores couple ferromagnetically to yield the experimentally observed triplet ground state. Crucially, despite short Ti···Ti distances of ∼3.3 Å, no significant direct metal−metal bonding or antiferromagnetic interactions appear to exist. This is in stark contrast to all known Ti^{III} dinuclear complexes with *planar* $Ti(\mu\text{-Cl})_2Ti$ rings, which even at Ti···Ti distances of ∼4.0 Å display significant antiferromagnetic interactions that yield singlet ground states. It is likely that in most cases this occurs via a direct exchange pathway resulting from, often very slight, Ti···Ti d-orbital overlap. In **3** and **4** the puckering of the $Ti(\mu\text{-Cl})_2Ti$ core reduces the effectiveness of this overlap and leaves paramagnetic superexchange as the dominant magnetic interaction between the metal centers, thereby yielding a triplet ground state.

■ ASSOCIATED CONTENT

Supporting Information

Crystallographic information files (CIFs) of complexes **2**−**4**; temperature dependence of the magnetic moment of **2** and parameters used to fit experimental data for **2**, **3**, and **4**; details of the DFT calculations, including absolute energies, optimized atom coordinates, Mulliken spin density plots and populations, and qualitative frontier molecular orbital diagrams. This material is available free of charge via the Internet at http://pubs.acs.org.

■ AUTHOR INFORMATION

Corresponding Authors

*E-mail: karl.wieghardt@cec.mpg.de.

*E-mail: ruediger.beckhaus@uni-oldenburg.de.

Present Address

[§]Division of Chemistry and Biological Chemistry, School of Physical and Mathematical Sciences, Nanyang Technological University, 21 Nanyang Link, Singapore 637371.

Notes

The authors declare no competing financial interest.

■ ACKNOWLEDGMENTS

J.E. is grateful to the Max-Planck Society for a postdoctoral fellowship

■ REFERENCES

(1) Gore-Randall, E.; Irwin, M.; Denning, M. S.; Goicoechea, J. M. *Inorg. Chem.* **2009**, *48*, 8304.

(2) In this Article, we adopt the following convention for the designation of 2,2′-bipyridine ligands (see Chart 1): (bpy) is used in a generic sense when no oxidation level of the ligand is specifically addressed; (bpy^0) is the neutral ligand ($S_L = 0$); $(bpy^{\bullet})^{1-}$ is the p-radical anion ($S_L = {}^1/_2$); $(bpy^{2-})^{2-}$ is its dianion ($S_L = 0$). An analogous nomenclature applies to 1,10-phenanthroline: (phen) when no oxidation state has been given, and $(phen^0)$, $(phen^{\bullet})^{1-}$, and $(phen^{2-})^{2-}$ when it has.

(3) (a) Irwin, M.; Jenkins, R. K.; Denning, M. S.; Krämer, T.; Grandjean, F.; Long, G. J.; Herchel, R.; McGrady, J. E.; Goicoechea, J. M. *Inorg. Chem.* **2010**, *49*, 6160. (b) Irwin, M.; Doyle, L. R.; Krämer, T.; Herchel, R.; McGrady, J. E.; Goicoechea, J. M. *Inorg. Chem.* **2012**, *51*, 12301.

(4) (a) Scarborough, C. C.; Wieghardt, K. *Inorg. Chem.* **2011**, *50*, 9773. (b) Scarborough, C. C.; Sproules, S.; Weyhermüller, T.; DeBeer, S.; Wieghardt, K. *Inorg. Chem.* **2011**, *50*, 12446. (c) Bowman, A. C.; Sproules, S.; Wieghardt, K. *Inorg. Chem.* **2012**, *51*, 3707. (d) England, J.; Scarborough, C. C.; Weyhermüller, T.; Sproules, S.; Wieghardt, K. *Eur. J. Inorg. Chem.* **2012**, 4605. (e) Bowman, A. C.; England, J.; Sproules, S.; Weyhermüller, T.; Wieghardt, K. *Inorg. Chem.* **2013**, *52*, 2242. (f) Wang, M.; England, J.; Weyhermüller, T.; Wieghardt, K. *Inorg. Chem.* **2014**, *53*, 2276.

(5) (a) McPherson, A. M.; Fieselmann, B. F.; Lichtenberger, D. L.; McPherson, G. L.; Stucky, G. D. *J. Am. Chem. Soc.* **1979**, *101*, 3425. (b) Bishop, L. A.; Turner, M. A.; Kool, L. B. *J. Organomet. Chem.* **1998**, *553*, 53.

(6) (a) Gyepes, R.; Witte, P. T.; Horáček, M.; Císařová, I.; Mach, K. *J. Organomet. Chem.* **1998**, *551*, 207. (b) Witte, P. T.; Klein, R.; Kooijman, H.; Spek, A. L.; Polášek, M.; Varga, V.; Mach, K. *J. Organomet. Chem.* **1996**, *519*, 195.

(7) Thewalt, U.; Berhalter, K. *J. Organomet. Chem.* **1986**, *302*, 193.

(8) Milko, P.; Iron, M. A. *J. Chem. Theory Comput.* **2014**, *10*, 220.

(9) Llinás, G. H.; Mena, M.; Palacios, F.; Royo, P.; Serrano, R. *J. Organomet. Chem.* **1988**, *340*, 37.

(10) Coutts, R. S. P.; Wailes, P. C.; Martin, R. L. *J. Organomet. Chem.* **1973**, *47*, 375.

(11) Jungst, R.; Sekutowski, D.; Davis, J.; Luly, M.; Stucky, G. *Inorg. Chem.* **1977**, *16*, 1645.

(12) Tupper, K. A.; Tilley, T. D. *J. Organomet. Chem.* **2005**, *690*, 1689.

(13) Liu, T.-F.; Feng, D.; Chen, Y.-P.; Zou, L.; Bosch, M.; Yuan, S.; Wei, Z.; Fordham, S.; Wang, K.; Zhou, H.-C. *J. Am. Chem. Soc.* **2015**, *137*, 413−419.

(14) Neese, F. *Orca, an Ab Initio Density Functional and Semiempirical Electronic Structure Program Package*, version 2.8, revision 2287; Universität Bonn: Bonn, Germany, 2010.

(15) (a) Becke, A. D. *Phys. Rev. A* **1988**, *38*, 3098. (b) Becke, A. D. *J. Chem. Phys.* **1993**, *98*, 5648. (c) Lee, C. T.; Yang, W. T.; Parr, R.G. *Phys. Rev. B* **1988**, *37*, 785.

(16) (a) Weigend, F.; Ahlrichs, R. *Phys. Chem. Chem. Phys.* **2005**, *7*, 3297. (b) Schäfer, A.; Huber, C.; Ahlrichs, R. *J. Chem. Phys.* **1994**, *100*, 5829. (c) Schäfer, A.; Horn, H.; Ahlrichs, R. *J. Chem. Phys.* **1992**, *97*, 2571.

DOI: 10.1021/acs.inorgchem.5b00285
Inorg. Chem. 2015, 54, 4811−4820

(17) (a) Eichkorn, K.; Weigend, F.; Treutler, O.; Ahlrichs, R. *Theor. Chem. Acc.* **1997**, *97*, 119. (b) Eichkorn, K.; Treutler, O.; Öhm, H.; Häser, M.; Ahlrichs, R. *Chem. Phys. Lett.* **1995**, *240*, 283. (c) Eichkorn, K.; Treutler, O.; Öhm, H.; Häser, M.; Ahlrichs, R. *Chem. Phys. Lett.* **1995**, *242*, 652.
(18) (a) Neese, F.; Wennmohs, F.; Hansen, A.; Becker, U. *Chem. Phys.* **2009**, *356*, 98. (b) Kossmann, S.; Neese, F. *Chem. Phys. Lett.* **2009**, *481*, 240. (c) Neese, F. *J. Comput. Chem.* **2003**, *24*, 1714.
(19) Grimme, S.; Antony, J.; Ehrlich, S.; Krieg, H. *J. Chem. Phys.* **2010**, *132*, 154104.
(20) (a) Noodleman, L. *J. Chem. Phys.* **1981**, *74*, 5737. (b) Noodleman, L.; Norman, J. G.; Osborne, J. H.; Aizman, A.; Case, D. *J. Am. Chem. Soc.* **1985**, *107*, 3418. (c) Noodleman, L.; Davidson, E. R. *Chem. Phys.* **1986**, *109*, 131. (d) Noodleman, L.; Case, D. A.; Aizman, A. J. *J. Am. Chem. Soc.* **1988**, *110*, 1001. (e) Noodleman, L.; Peng, C. Y.; Case, D. A.; Monesca, J. M. *Coord. Chem. Rev.* **1995**, *144*, 199.
(21) Neese, F. *J. Phys. Chem. Solids* **2004**, *65*, 781.
(22) Pettersen, E. F.; Goddard, T. D.; Huang, C. C.; Couch, G. S.; Greenblatt, D. M.; Meng, E. C.; Ferrin, T. E. *J. Comput. Chem.* **2004**, *25*, 1605.
(23) Preuss, K. E. *Polyhedron* **2014**, *79*, 1.
(24) (a) Mulliken, R. S.; Person, W. B. *Molecular Complexes*; Wiley & Sons: New York, 1969; Chapter 16. (b) Suzuki, S.; Morita, Y.; Fukui, K.; Sato, K.; Shiomi, D.; Takui, T.; Nakasuji, K. *J. Am. Chem. Soc.* **2006**, *128*, 2530.
(25) König, E.; Herzog, S. *J. Inorg. Nucl. Chem.* **1970**, *32*, 613.
(26) Wang, M.; Weyhermüller, T.; England, J.; Wieghardt, K. *Inorg. Chem.* **2013**, *52*, 12763.
(27) Wang, M.; Weyhermüller, T.; Wieghardt, K. Submitted.
(28) Lukens, W. W., Jr.; Andersen, R. A. *Inorg. Chem.* **1995**, *34*, 3440.
(29) (a) Soda, T.; Kitagawa, Y.; Onishi, T.; Takano, Y.; Shigeta, Y.; Nagao, H.; Yoshioka, Y.; Yamaguchi, K. *Chem. Phys. Lett.* **2000**, *319*, 223. (b) Yamaguchi, K.; Takahara, Y.; Fueno, T. *Applied Quantum Chemistry*; Smith, V. H., Ed.; Reidel: Dordrecht, Netherlands, 1986; p 155.
(30) Sung, R. C. W.; Courtenay, S.; McGarvey, B. R.; Stephan, D. W. *Inorg. Chem.* **2000**, *39*, 2542.
(31) (a) DeKock, R. L.; Peterson, M. A.; Reynolds, L. E. L.; Chen, L.-H.; Baerends, E. J.; Vernooijs, P. *Organometallics* **1993**, *12*, 2794. (b) Bénard, M.; Rohmer, M.-M. *J. Am. Chem. Soc.* **1992**, *114*, 4785.

DOI: 10.1021/acs.inorgchem.5b00285
Inorg. Chem. 2015, 54, 4811−4820